

Reflection and transmission of a compression wave at a tunnel portal

M.S. Howe^{a,*}, E.A. Cox^b

^a*Boston University, College of Engineering, 110 Cummington Street, Boston, MA 02215, USA*

^b*Mathematical Physics Department, University College Dublin, Dublin 4, Ireland*

Received 9 December 2004; accepted 2 May 2005

Abstract

Analyses are made of the interaction of the nonlinearly steepened, compression wavefront generated by a high-speed train in a tunnel with the tunnel portal ahead of the train. The ‘micro-pressure’ pulse emitted from the portal can rattle structures in nearby buildings, and the expansion wave reflected back towards the train can cause discomfort to passengers. It is concluded that the usual simplified approximation of one-dimensional propagation within the tunnel provides an adequate representation of interactions of the wave with the portal, and also with ‘windows’ in the tunnel wall near the portal. It is shown how a discrete distribution of windows can be used to produce a reflected expansion wave that varies linearly across the wavefront, and how the thickness of that wavefront can be made many times larger than the thickness of the incident compression wave profile. A detailed analysis of the wave radiated from the portal reveals that cumulative nonlinear effects of propagation over long distances make little or no contribution to the free-space radiation of the micro-pressure wave.

© 2005 Elsevier Ltd. All rights reserved.

Keywords: High-speed train; Micro-pressure wave; Tunnel hoods; KZK-equation; Cummings equation

1. Introduction

Low-frequency, large-amplitude pressure waves are generated in tunnels when trains enter and leave the tunnel, and when trains within the tunnel pass geometrical features such as changes in cross-sectional area or meet an oncoming train. The amplitude of the compression wave generated by a high-speed train entering a tunnel at speed $U > 250$ km/h, say, typically exceeds 1.5–2 kPa. Multiple reflections of waves from tunnel discontinuities can create localized regions where constructive interference produces much higher pressures that can cause discomfort to passengers and railway personnel within the tunnel. In long tunnels nonlinear steepening of a wavefront can greatly increase the amplitude of the wave (called the ‘micro-pressure wave’) subsequently radiated from the far end of the tunnel when the compression wave arrives (Maeda, 2002).

Various tunnel portal modifications and ‘hoods’ (tunnel extensions) are used, principally in Japan, to greatly increase the rise time of the compression wave generated by an entering train (Ozawa et al., 1978; Ozawa and Maeda, 1988a, b). This tends to inhibit ‘shock’ formation by nonlinear steepening in a long tunnel, and thereby reduce the impact of the

*Corresponding author. Tel.: +1 617 484 0656; fax: +1 617 353 5866.

E-mail address: mshowe@bu.edu (M.S. Howe).

micro-pressure wave, whose amplitude is proportional to the slope of the compression wavefront impinging on the tunnel exit. A hood consists of a cylindrical tunnel extension typically up to 50 m long (Maeda, 2002) with a set of windows distributed along its sides or in the roof, from which high-pressure air produced by an entering train can escape. Proper choice of window sizes and spacings can produce a greatly elongated, smoothly growing compression wavefront.

However, the presence of tunnel portal modifications also changes the way that a compression wave incident from within the tunnel is reflected and transmitted at the portal. The likely practical importance of the modified reflection problem was noted by Vardy (1978), and more recently by Brown and Vardy (1994). Vardy (1978) examined reflection from flared and homogeneously perforated portals, by a modified form of the method of characteristics for an incident wave of step-wave profile. The problem was investigated numerically and experimentally by Brown and Vardy (1994); an analytical procedure was also developed by means of an approximate extension of the Levine and Schwinger (1948) theory of the radiation of sound from the open end of a thin-walled circular cylinder, and by a similar application of the corresponding solution due to Chester (1950) for a portal opening into a two-dimensional ‘cutting’.

The more general question of the interaction of sound and shock waves with the open end of a smooth-walled duct has been examined extensively. The circular cylindrical duct is discussed analytically by Morse and Feshbach (1953) and Noble (1958); Rudinger (1955, 1957) has investigated experimentally shock wave reflection from the exit; the acoustic problem with and without mean flow has been examined by van Wijngaarden (1968), van Wijngaarden and Disselhorst (1979), Disselhorst and van Wijngaarden (1980) and by Peters et al. (1993). Applications of approximate forms of the linear theory (valid for frequencies not exceeding the first ‘cut-off’ frequency of the duct) to the micro-pressure wave problem are discussed by Ozawa et al. (1978, 1997).

In this paper theoretical understanding of compression wave reflection and transmission at a tunnel portal is extended by means of an explicit analysis of the influence of a distribution of discrete windows near the exit, and by consideration of the likely effects of acoustic nonlinearity outside the tunnel on the micro-pressure wave. The problem is formulated in Section 2 in terms of the usual linear theory of a compression wave incident on an open end. The subsequent free-space development of the micro-pressure wave is examined in Section 3 by application of the nonlinear ‘parabolic’ approximation to study nonlinear propagation over large distances. The influence of windows on the expansion wave reflected back into the tunnel is discussed in Section 4.

2. Formulation

2.1. The incident wave

Compression wave experiments are usually performed at model scale using a highly simplified tunnel geometry. We shall consider the simplest such configuration where the tunnel is in the form of a thin walled, nominally rigid circular cylindrical duct. For the purpose of analysis it is sufficient to consider a duct of semi-infinite length of radius R , whose axis extends along the negative x -axis, with the origin of coordinates $\mathbf{x} = (x, y, z)$ taken at O in the centre of the open end, as illustrated in Fig. 1. This simple model will be modified in Section 4 to include a set of windows in the tunnel wall distributed with centroids along a line parallel to the tunnel axis.

The incident plane compression wave of pressure $p_I(t - x/c_0)$ will be regarded as a steepened step wavefront across which the pressure rises to a maximum over an axial distance $\sim 2\delta$, as indicated in the figure, where t denotes time and c_0 is the undisturbed sound speed. Although the wave is assumed to have experienced steepening during propagation through the tunnel prior to its incidence on the exit portal, the wave amplitude \bar{p} , say, is in practice no more than about

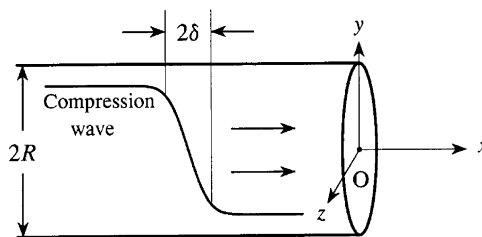


Fig. 1. Configuration of the circular cylindrical tunnel portal of radius R , the coordinate axes, and the incident compression wave.

2–3% of atmospheric pressure, and we can safely ignore nonlinear distortion of the wave within the tunnel over propagation distances of several tunnel diameters near the portal.

To fix ideas, the incident step wave shown in Fig. 1 is taken in the form

$$p_I = \frac{\bar{p}}{2} \left[1 + \operatorname{erf} \left(\frac{t - x/c_0}{\tau} \right) \right], \quad \tau \equiv \delta/c_0 = \text{constant}, \quad x < 0, \quad (2.1)$$

where $\operatorname{erf}(x) = (2/\sqrt{\pi}) \int_0^x e^{-\xi^2} d\xi$ is the error function (Abramowitz and Stegun, 1970). It will also be convenient to introduce the Fourier time transform $\hat{p}_I(\omega)$ of this wave

$$\hat{p}_I(\omega) = \frac{-\bar{p}}{2\pi i} \frac{e^{-\omega^2 \tau^2/4}}{(\omega + i0)}, \quad (2.2)$$

in terms of which

$$p_I = \int_{-\infty}^{\infty} \hat{p}_I(\omega) e^{-i\omega(t-x/c_0)} d\omega, \quad x < 0. \quad (2.3)$$

The notation ‘i0’ in Eq. (2.2) indicates that the integration contour in Eq. (2.3) is required to pass *above* the pole at $\omega = 0$. Definition (2.1) implies that the compression wave arrives at the open end at time $t \sim 0$.

At full scale, measured values of the compression wave semi-thickness δ at the exit portal are rarely smaller than about $0.5R$, even in the absence of countermeasures designed to inhibit wave steepening in the tunnel (Iida, 2003) (the pressure rise experienced by a stationary observer in the tunnel then occurs over a time ~ 0.03 s). Effective countermeasures usually ensure that $\delta > 3R$, where typically $R \sim 6$ m at train speeds of, say, 300 km/h.

2.2. Diffraction at the open end

The irrotational interaction of a linear acoustic wave with the open end of a rigid, circular duct can be evaluated exactly (Noble, 1958). Consider a single harmonic component $e^{-i\omega(t-x/c_0)}$ of the step wave (2.1), and temporarily suppress the time factor $e^{-i\omega t}$. If this element of the incident wave is written $e^{ik_0 x}$, where $k_0 = \omega/c_0$ is the acoustic wave number, the overall acoustic pressure is given by Noble (1958) in the form

$$p = \frac{k_0 R K_+(k_0)}{2\pi i} \int_{-\infty}^{\infty} \frac{K_-(k) K_0(\gamma r) e^{ikx} dk}{\gamma K_1(\gamma R)}, \quad \text{for } r = \sqrt{y^2 + z^2} > R, \quad (2.4)$$

$$= e^{ik_0 x} - \frac{k_0 R K_+(k_0)}{2\pi i} \int_{-\infty}^{\infty} \frac{K_-(k) I_0(\gamma r) e^{ikx} dk}{\gamma I_1(\gamma R)}, \quad \text{for } r < R. \quad (2.5)$$

In these formulae I_ν , K_ν are modified Bessel functions (Abramowitz and Stegun, 1970); the function $\gamma \equiv \gamma(k) = \sqrt{k^2 - k_0^2}$ is defined with branch cuts extending, respectively, from $k = \pm k_0$ to $\pm i\infty$, such that for real values of k

$$\gamma = |k^2 - k_0^2|^{1/2} \text{ for } |k| > |k_0|, \quad \text{and} \quad \gamma = -i \operatorname{sgn}(k_0) |k_0^2 - k^2|^{1/2} \text{ for } |k| < |k_0|, \quad (2.6)$$

where the positive square roots are taken. The functions $K_\pm(k)$ are, respectively, regular and nonzero in $\operatorname{Im} k \geq 0$, and satisfy

$$K_+(k) K_-(k) = K(k) \equiv 2K_1(\gamma R) I_1(\gamma R). \quad (2.7)$$

In addition

$$K_-(-k) = K_+(k), \quad K_\pm(0) = 1, \quad \{K_+(k)\}_{-k_0} = \text{c.c.} \{K_+(k)\}_{+k_0}, \quad (2.8)$$

where ‘c.c.’ denotes ‘complex conjugate’, and

$$K_+(k) = \sqrt{K(k)} \exp \left\{ \frac{k}{\pi i} \int_0^\infty \frac{\ln[K(\xi)/K(k)] d\xi}{\xi^2 - k^2} \right\}, \quad \text{for } \operatorname{Im} k = 0, \quad (2.9)$$

$$= \exp \left\{ \frac{1}{2\pi i} \int_{-\infty}^\infty \frac{\ln[K(\xi)] d\xi}{\xi - k} \right\}, \quad \text{for } \operatorname{Im} k > 0. \quad (2.10)$$

2.3. Free space radiation

At distances $|\mathbf{x}| \gg 1/k_0$ from the open end in the exterior, free space region, integral (2.4) can be evaluated by the method of stationary phase to yield

$$p \sim - \frac{iR}{|\mathbf{x}|} \frac{J_1(k_0 R \sin \theta)}{\sin \theta} \frac{K_+(k_0) e^{ik_0 |\mathbf{x}|}}{K_+(k_0 \cos \theta)}, \quad |\mathbf{x}| \rightarrow \infty, \tag{2.11}$$

where J_1 is the Bessel function of order 1, and θ is the angle between the radiation direction \mathbf{x} and the positive x -axis.

The corresponding far field representation for the incident wave (2.2) is obtained by multiplying the right-hand side of Eq. (2.11) by $\hat{p}_I(\omega)$, restoring the time factor $e^{-i\omega t}$ and integrating over $-\infty < \omega < \infty$:

$$p \sim - \frac{iR}{|\mathbf{x}|} \int_{-\infty}^{\infty} \frac{J_1(k_0 R \sin \theta)}{\sin \theta} \frac{K_+(k_0)}{K_+(k_0 \cos \theta)} \hat{p}_I(\omega) e^{-i\omega(t-|\mathbf{x}|/c_0)} d\omega, \quad |\mathbf{x}| \rightarrow \infty. \tag{2.12}$$

For an incident step wave of large rise time $\tau \gg R/c_0$ the Fourier transform $\hat{p}_I(\omega)$ is small except when $\omega R/c_0 \equiv k_0 R \ll 1$, and Eq. (2.12) can be approximated by replacing the non-exponential terms in the integrand by their limiting values as $k_0 R \rightarrow 0$ (when $J_1(k_0 R \sin \theta) \sim \frac{1}{2} k_0 R \sin \theta$ and $K_+(k_0)/K_+(k_0 \cos \theta) \sim 1$). This yields the well-known monopole approximation

$$p \sim \frac{\mathcal{A}}{2\pi c_0 |\mathbf{x}|} \frac{\partial p_I}{\partial t}(t - |\mathbf{x}|/c_0), \quad |\mathbf{x}| \rightarrow \infty, \tag{2.13}$$

where $\mathcal{A} = \pi R^2$ is the cross-sectional area of the duct. This formula can also be expressed in terms of the acoustic particle velocity v_I , say, of the incident wave, which satisfies

$$v_I(t - x/c_0) = \frac{p_I(t - x/c_0)}{\rho_0 c_0}, \quad x < 0, \tag{2.14}$$

where ρ_0 is the mean air density, i.e.

$$p \sim \frac{\rho_0 \mathcal{A}}{2\pi |\mathbf{x}|} \frac{\partial v_I}{\partial t}(t - |\mathbf{x}|/c_0), \quad |\mathbf{x}| \rightarrow \infty. \tag{2.15}$$

Approximations (2.13) and (2.15) are also applicable for *arbitrary* incident wave thickness for sound radiated directly out of the tunnel along the axial direction (the positive x -axis), because

$$\frac{J_1(k_0 R \sin \theta)}{\sin \theta} \frac{K_+(k_0)}{K_+(k_0 \cos \theta)} \rightarrow \frac{k_0 R}{2} \quad \text{as } \theta \rightarrow 0.$$

Further, also for arbitrary compression wave thickness, the radiation along the x -axis is exactly equal to that produced if the unflanged duct opening is replaced by a circular piston of area \mathcal{A} vibrating at small amplitude velocity $v_I(t)$ in an infinite plane baffle (Morse and Feshbach, 1953; Rayleigh, 1926). This conclusion motivates the analysis given below in Section 3 (involving a *baffled* opening) to examine the importance of nonlinearity on the micro-pressure wave radiated from a tunnel portal. For the step wave (2.1) the corresponding piston velocity is

$$v_I = \frac{\bar{p}}{2\rho_0 c_0} [1 + \text{erf}(t/\tau)], \quad \tau \equiv \delta/c_0. \tag{2.16}$$

2.4. Wave reflected in the tunnel

The integrand of the time-harmonic solution (2.5) is regular except for poles in $\text{Im } k < 0$. The residue theorem may therefore be used to express the overall pressure wave p_R reflected back into the tunnel in the form

$$p_R = - \sum_{n=0}^{\infty} \int_{-\infty}^{\infty} \frac{\hat{p}_I(\omega) k_0 K_+(k_0) K_+(k_n) J_0(j_n r/R)}{k_n J_0(j_n)} e^{-i(\omega t + k_n x)} d\omega, \quad x < 0, \quad r < R, \tag{2.17}$$

where J_0, J_1 are Bessel functions (Abramowitz and Stegun, 1970), $j_0 = 0, j_n (n > 0)$ is the n th positive zero of $J_1(z)$, and

$$k_n R = \text{sgn}(k_0) |k_0^2 R^2 - j_n^2|^{1/2} \quad \text{for } |k_0 R| > j_n, \quad k_n R = i |j_n^2 - k_0^2 R^2|^{1/2} \quad \text{for } |k_0 R| < j_n. \tag{2.18}$$

Series (2.17) represents an expansion wave whose wavefront is determined by the first term ($n = 0$), which is the only term of plane wave form in the reflected disturbance, and propagates parallel to the tunnel axis at the speed of sound.

For the incident compression wave (2.1), the overall pressure in the vicinity of the expansion wavefront is therefore given by

$$p = p_I(t - x/c_0) + \frac{\bar{p}}{2\pi i} \int_{-\infty}^{\infty} \frac{\{K_+(k_0)\}^2}{k_0 + i0} e^{-ik_0 c_0(t+x/c_0) - k_0^2(c_0\tau)^2/4} dk_0, \quad \text{near } t + x/c_0 \sim 0. \quad (2.19)$$

In this formula

$$\mathcal{R} = -\{K_+(k_0)\}^2 \equiv -|K_+(k_0)|^2 e^{-2ik_0\ell'} \quad (2.20)$$

is the plane wave reflection coefficient for waves of frequency ω , and ℓ' is the ‘end correction’ $\sim 0.61R$ when $k_0R \rightarrow 0$ (Rayleigh, 1926).

The integral in Eq. (2.19) is computed numerically by first evaluating the corresponding integral for $\partial p/\partial t$, for which the integrand is finite at $k_0 = 0$, and then using

$$p = p_I + \int_{-\infty}^{t+x/c_0} \frac{\partial p}{\partial t} dt.$$

The results of such a calculation are depicted in Fig. 2 by the solid-line wave profiles (—), where the expansion wavefronts p/\bar{p} are plotted against $c_0(t + x/c_0)/R$ for three incident step waves with $\delta/R = 0.1, 0.5, 1$. The wave

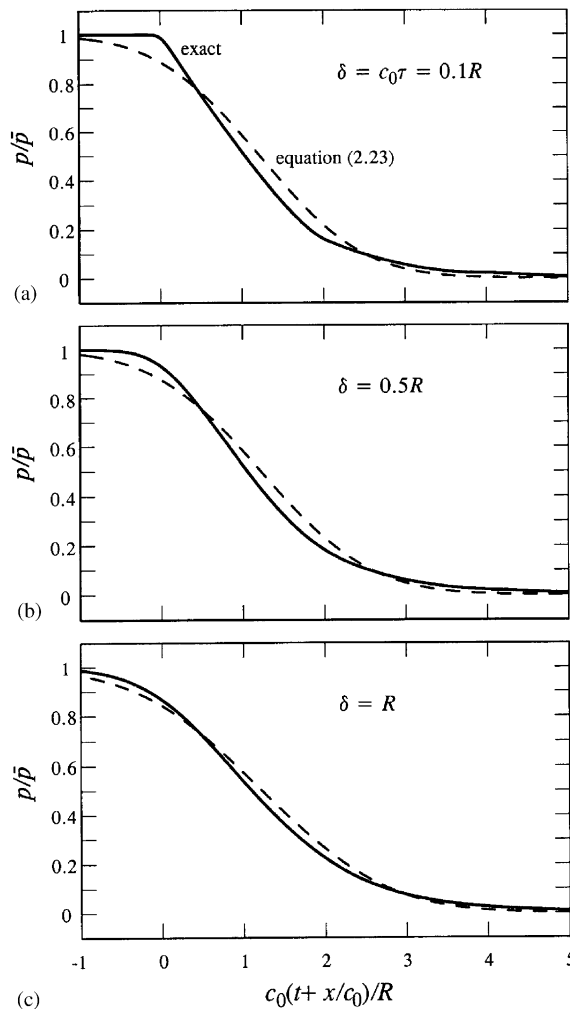


Fig. 2. Pressure variation at the reflected wavefront in the tunnel: —, exact solution (2.19); - - -, approximation (2.23): (a) $\delta/R = 0.1$, (b) 0.5, (c) 1.

profiles are practically identical except in the immediate vicinities of the front of the expansions, where the details depend on the precise arrival time of the head of the compression wave at the open end of the duct. In all cases the overall width of the expansion wave $\sim 2R$, irrespective of the width 2δ of the incident wave. This is because, to a good approximation, for these values of δ/R the low-frequency content of the three incident waves are essentially identical, and it is only the low-frequency components of the incident waves that are effectively reflected at the exit.

It is interesting to compare these predictions with the corresponding results obtained in the low-frequency approximation, where all relevant values of the wave number k_0 in the integral of Eq. (2.19) satisfy $k_0R \ll 1$. In that case we can use the plane wave reflection model described by Lighthill (1978) (Chapter 2), according to which the acoustic admittance Y_E of the open end of the cylinder can be approximated by

$$Y_E = \frac{i\mathcal{A}}{\rho_0 c_0} \cot\left(\frac{\chi}{2}\right), \quad \text{where } \chi = k_0 \ell_E + \frac{ik_0^2 \mathcal{A}}{4\pi}. \tag{2.21}$$

In this formula ℓ_E is the end correction as $k_0R \rightarrow 0$, and the imaginary part of χ represents the effect of radiation from the open end.

Standard manipulations discussed by Lighthill (1978) show that the reflection coefficient for a time harmonic wave e^{ik_0x} (corresponding to Eq. (2.20) above) is given in terms of Y_E by

$$\mathcal{R} = -\left(\frac{\mathcal{A}/\rho_0 c_0 - Y_E}{\mathcal{A}/\rho_0 c_0 + Y_E}\right) = -e^{i\chi}. \tag{2.22}$$

Hence, the reflected wave p_R (corresponding to the integrated term in Eq. (2.19)) becomes

$$\begin{aligned} p_R &= -\frac{\bar{p}}{2\pi i} \int_{-\infty}^{\infty} e^{-ik_0 c_0(t+x/c_0-2\ell_E)-k_0^2((c_0 t)^2+2R^2)/4} \frac{dk_0}{k_0+i0} \\ &= -\frac{\bar{p}}{2} \left\{ 1 + \operatorname{erf}\left(\frac{c_0 t + x - 2\ell_E}{\sqrt{\delta^2 + 2R^2}}\right) \right\}. \end{aligned} \tag{2.23}$$

The broken line curves in Fig. 2 indicate that this formula may be regarded as accurate for an incident step wave with $\delta \geq R$, and that it provides an acceptable approximation of the expansion wave for $\delta = 0.5R$. In all practical applications of these results, δ lies in the range where the plane wave approximation is valid.

3. Influence of nonlinearity on the micro-pressure wave

3.1. The piston model

The baffled piston model discussed in Section 2.3 will now be used to estimate the effect of nonlinearity on the free space propagation of the micro-pressure wave. The nonlinearly steepened compression wavefront incident on the tunnel exit is then regarded as an acoustic beam radiating from an axisymmetric source at $x = 0$, whose subsequent evolution outside the tunnel is governed in a first approximation by the parabolic KZK equation (Zabolotskaya and Khokhlov, 1969; Kuznetsov, 1971). In terms of axisymmetric cylindrical coordinates (x, r) , the pressure $p(x, r, t)$ propagates according to the following form of the KZK equation:

$$\frac{\partial}{\partial t'} \left(\frac{\partial p}{\partial x} - \frac{\Gamma}{\rho_0 c_0^3} p \frac{\partial p}{\partial t'} - \frac{\nu}{2c_0^3} \frac{\partial^2 p}{\partial t'^2} \right) = \frac{c_0}{2} \left(\frac{\partial^2 p}{\partial r^2} + \frac{1}{r} \frac{\partial p}{\partial r} \right), \tag{3.1}$$

where $t' = t - x/c_0$, and Γ, ν are, respectively, the coefficient of nonlinearity and the acoustic diffusivity, given by

$$\Gamma = \frac{\gamma + 1}{2}, \quad \nu = \frac{1}{\rho_0} \left[\eta' + \frac{4\eta}{3} + \kappa \left(\frac{1}{c_v} - \frac{1}{c_p} \right) \right],$$

$\gamma = c_p/c_v$ being the ratio of the specific heats at constant pressure and density, κ the thermal conductivity and η, η' are, respectively, the shear and bulk coefficients of viscosity. We also have $\rho_0 c_0^2 = \gamma p_0$ where p_0 is the mean air pressure.

Outside the portal the axis of the acoustic beam lies along the x direction from which r represents the transverse radial distance. The parabolic approximation (3.1) is strictly applicable in the region of the wavefront, in the neighbourhood of which it may be assumed that transverse variations of the acoustic pressure are slow compared to variations in the direction of the acoustic axis. Within this approximation the KZK equation retains the influences of nonlinear distortion, thermoviscous diffusion and weak diffraction of the wavefront.

Eq. (3.1) is usually cast in nondimensional form by setting

$$\tilde{p} = \frac{p}{\bar{p}}, \quad \tilde{r} = \frac{r}{R}, \quad \tilde{x} = \frac{x}{R/2}, \quad \tilde{t} = \frac{c_0 t'}{R}, \tag{3.2}$$

in terms of which Eq. (3.1) becomes

$$\frac{\partial}{\partial \tilde{t}} \left(\frac{\partial \tilde{p}}{\partial \tilde{x}} - \tilde{\Gamma} \tilde{p} \frac{\partial \tilde{p}}{\partial \tilde{t}} - \tilde{v} \frac{\partial^2 \tilde{p}}{\partial \tilde{t}^2} \right) = \frac{1}{4} \left(\frac{\partial^2 \tilde{p}}{\partial \tilde{r}^2} + \frac{1}{\tilde{r}} \frac{\partial \tilde{p}}{\partial \tilde{r}} \right), \tag{3.3}$$

where

$$\tilde{v} = \frac{v}{4Rc_0}, \quad \tilde{\Gamma} = \frac{\gamma + 1}{4\gamma} \left(\frac{\bar{p}}{p_0} \right) \tag{3.4}$$

and $\gamma = 1.4$ for air.

The following further change of variables [first proposed in an analysis of periodic waves by Hamilton et al. (1985)] facilitates numerical integration into the far field:

$$P = (1 + \tilde{x})\tilde{p}, \quad s = \frac{\tilde{r}}{1 + \tilde{x}}, \quad T = \tilde{t} - \frac{\tilde{r}^2}{1 + \tilde{x}}. \tag{3.5}$$

In the far field ($\tilde{x} \gg 1$) in radiation directions making a small angle θ with the beam axis, we have $s = \frac{1}{2}r/x = \frac{1}{2}\tan\theta$ and $RT/c_0 = t - x/c_0 - r^2/2c_0x$. Therefore, constant values of s correspond in the far field to constant radiation angles θ and constant values of T correspond to wavefront surfaces. The decrease in the amplitude of \tilde{p} caused by spreading of the wavefront is conveniently removed by transforming to the normalized pressure P , which is found to satisfy

$$\frac{\partial}{\partial T} \left(\frac{\partial P}{\partial \tilde{x}} - \frac{\tilde{\Gamma}}{1 + \tilde{x}} P \frac{\partial P}{\partial T} - \tilde{v} \frac{\partial^2 P}{\partial T^2} \right) = \frac{1}{4(1 + \tilde{x})^2} \left(\frac{\partial^2 P}{\partial s^2} + \frac{1}{s} \frac{\partial P}{\partial s} \right). \tag{3.6}$$

The solution of this equation is required subject to the ‘piston source’ boundary condition (2.16) imposed at $x = 0$. This condition strictly models a circular piston of radius R vibrating in an infinite plane baffle, although the effect of the baffle on the evolution of the sharp wavefront should be negligible at high frequencies. When expressed in terms of the transformed variables, the boundary condition for $P(\tilde{x}, s, T)$ becomes

$$P(0, s, T) = \begin{cases} \frac{1}{2} \left[1 + \operatorname{erf} \left(\frac{R}{\delta} (T + s^2) \right) \right], & 0 \leq s \leq 1, \\ 0, & s > 1. \end{cases} \tag{3.7}$$

At any point in the acoustic field the solution of Eq. (3.6) vanishes for $T < T_L$, where T_L is sufficiently large and negative that the pulse from the portal has not arrived. Hence, integration of Eq. (3.6) supplies

$$\frac{\partial P}{\partial \tilde{x}} - \frac{\tilde{\Gamma}}{1 + \tilde{x}} P \frac{\partial P}{\partial T} - \tilde{v} \frac{\partial^2 P}{\partial T^2} = \frac{1}{4(1 + \tilde{x})^2} \int_{T_L}^T \left(\frac{\partial^2 P}{\partial s^2} + \frac{1}{s} \frac{\partial P}{\partial s} \right) dT. \tag{3.8}$$

This is solved by constructing a computational grid for $T_L < T < T_U$ and $0 < s < s_U$, say, with the pulse propagating in the direction of increasing \tilde{x} subject to initial condition (3.7) at $\tilde{x} = 0$. At the edges of the computational grid $P = 0$, except at $s = 0$ where symmetry demands that $\partial P / \partial s = 0$. The values of T_L, T_U, s_U are chosen to avoid reflections from the artificial boundaries. The numerical procedure uses a four-point upwinded explicit finite-difference scheme for the nonlinear term. The diffraction term is modelled in the near field, up to $\tilde{x} = 0.1$, by a fully implicit backward difference method; for larger \tilde{x} a Crank–Nicolson method was used (Lee and Hamilton, 1995). The integral was evaluated using the trapezoidal rule.

3.2. The micro-pressure wave

Calculated micro-pressure wave profiles (expressed in terms of the normalized pressure P) just outside the portal are illustrated in Fig. 3 for $x = R$ and for transverse radial distances $r = 0, R, 2R, 3R$ when the incident compression wave strength $\bar{p} = 4$ kPa and the semi-thickness $\delta = 0.5R$. Acoustic nonlinearity is negligible in the near field, and the profiles displayed in this figure correspond to the usual predictions of the linear theory of diffraction of high-frequency sound emerging from a long tube (Ozawa et al., 1978; Levine and Schwinger, 1948; Morse and Feshbach, 1953; Noble, 1958), according to which there is rapid off-axis attenuation of the signal (with increasing values of r) accompanied by a characteristic broadening of the wavefront.

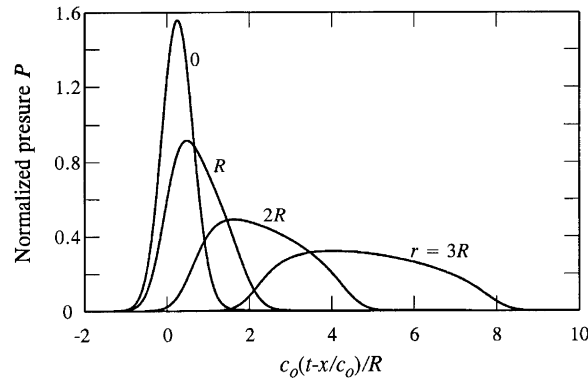


Fig. 3. Profiles of the propagating micro-pressure wave P normalized as in Eq. (3.5) and calculated from Eq. (3.8) using the initial condition (3.7). The compression wave amplitude $\bar{p} = 4$ kPa, semi-thickness $\delta = 0.5R$ and the acoustic diffusivity $\bar{\nu} = 10^{-6}$. The solutions are constructed at an axial distance of one tunnel radius from the portal exit plane at transverse distances $r = 0, R, 2R, 3R$.

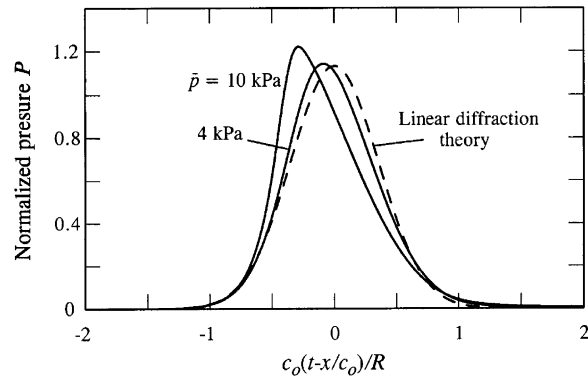


Fig. 4. Influence of nonlinearity on the far field form of the micro-pressure wave P normalized as in Eq. (3.5) and calculated from Eq. (3.8) using the initial condition (3.7). Solutions are constructed on the exterior tunnel axis ($r = 0$) at $x = 172R$ for $\bar{p} = 4$ and 10 kPa when $\delta = 0.5R$ and $\bar{\nu} = 10^{-6}$.

Nonlinear distortion of the micro-pressure wave is likely to be important only at large distances from the portal, and then principally in radiation directions along the exterior tunnel axis. However, the calculated results shown in Fig. 4 for $r = 0$ reveal that for x as large as $172R$ nonlinearity appears to play a relatively minor role in modifying the profile of the micro-pressure wave. The wave profile when the incident compression wave amplitude $\bar{p} = 4$ kPa (typical of trains travelling at speeds in excess of about 360 km/h) differs only very marginally from that predicted by linear acoustics (the broken line curve in the figure). Wavefront steepening is still seen to be of marginal significance even when \bar{p} is increased to 10 kPa, which is very much larger than any compression wave amplitude encountered in practice.

4. Influence of windows on the reflected wave

4.1. Jet formation at the windows

A window in the wall of a tunnel portal (Fig. 5) behaves as a pressure node at very low frequencies, at which an incident pressure rise within the tunnel is opposed by the production of an equal and opposite expansion wave which propagates away from the window in both directions within the tunnel. The situation is different, however, at the higher frequencies associated with a steepened compression wave p_I , because the inertial reaction of air forced through a

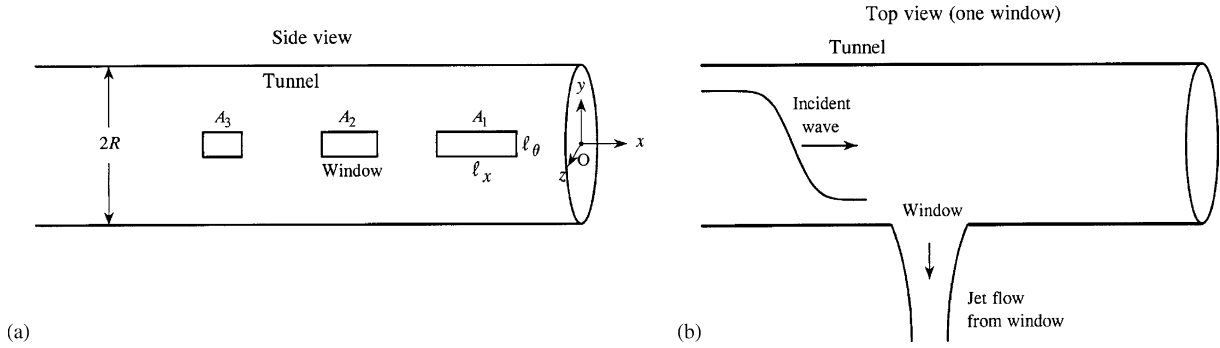


Fig. 5. (a) Circular cylindrical tunnel portal with rectangular windows; (b) air flow from a window.

window is no longer negligible (Howe et al., 2003; Howe, 2005). The pressure fluctuations produced by the compression wave have a time scale $\sim R/c_0$, and the corresponding compression wavefront semi-thickness $\sim \delta$ is typically of the same order as a window diameter, or slightly larger. Therefore, it is usually possible to assume that the local tunnel pressure is uniform over the inner face of a window, and this approximation will be made in the following. This will not be true for very elongated windows, however, but they can be modelled analytically by a distribution of adjacent, smaller windows. Under these circumstances the air flow through the windows can be calculated using a set of empirical equations proposed and validated experimentally by Cummings (1984, 1986) for circular apertures.

Suppose there are N windows distributed in the manner illustrated in Fig. 5(a) along the side wall of the tunnel portal. Consider the motion through the k th window of area \mathcal{A}_k whose geometric centroid is at $x = x_k < 0$. A uniform pressure load $p(t)$ within the tunnel causes air to flow through the window forming a jet (Fig. 5(b)); the pressure load outside the tunnel is assumed to be negligible. Let $V_k(t)$ denote the mean jet velocity in the plane of the window directed out of the tunnel. Then (Cummings, 1984, 1986)

$$\bar{\ell}_k(t)\rho_0 \frac{dV_k}{dt} + \frac{\rho_0 V_k |V_k|}{2\sigma^2} = p(t), \tag{4.1}$$

where σ is a jet ‘contraction ratio’ and $\bar{\ell}_k(t)$ is a time-dependent window end-correction. For irrotational flow through the window (no jet formation)

$$\bar{\ell}_k(t) \approx \ell_w + 2\ell_0,$$

where $\ell_0 \approx \pi R_k/4$ is the end-correction of the window-opening on either side of the tunnel wall, $R_k = \sqrt{\mathcal{A}_k/\pi}$ is the equivalent radius of the window, and ℓ_w is the wall thickness of the tunnel (Rayleigh, 1926). For the real flow $\bar{\ell}_k(t)$ depends on jet length

$$\mathcal{L}_k(\tau) = \int_0^\tau |V_k(t)| dt, \tag{4.2}$$

where the time τ is measured from the instant at which $V_k(t)$ last changed sign. Then (Cummings, 1984, 1986)

$$\bar{\ell}_k(t) = \frac{\pi R_k}{4} + \left(\ell_w + \frac{\pi R_k}{4} \right) \left/ \left[1 + \frac{1}{3} \left(\frac{\mathcal{L}_k}{2R_k} \right)^{1.585} \right] \right. \tag{4.3}$$

The contraction ratio σ in Eq. (4.1) can be assumed to be constant to a good approximation. For unsteady flow $\sigma = 0.75$ yields predictions that accord well with experiment (Cummings, 1984, 1986; Howe, 2005), and this value is used below.

We assume one-dimensional (axial) wave propagation within the tunnel. Then, the volume velocity $V_k(t)\mathcal{A}_k$ of the flow out of the window generates two equal plane acoustic waves propagating in both directions away from the window. Before any further interactions occur between these waves and the tunnel exit or with any other windows, they produce a pressure fluctuation within the tunnel equal to

$$-\frac{\rho_0 c_0 \mathcal{A}_k}{2\mathcal{A}} V_k \left(t - \frac{|x - x_k|}{c_0} \right). \tag{4.4}$$

If we temporarily ignore the presence of other windows, we can account for the open end of the tunnel, where the net perturbation pressure must vanish at $x = \ell_E$, by introducing an ‘image’ window with centroid at $x = -x_k + 2\ell_E$ with

mean flow velocity equal to $-V_k(t)$. The pressure $p_k(x, t)$ within the tunnel attributable to the k th window and its image can then be cast in the form

$$p_k(x, t) = -\frac{\rho_0 c_0 \mathcal{A}_k}{2\mathcal{A}} \left\{ V_k \left(t + \frac{|x - x_k|}{c_0} \right) - V_k \left(t + \frac{|x + x_k - 2\ell_E|}{c_0} \right) \right\}. \tag{4.5}$$

This formula is equivalent to using the long wavelength approximation (2.22) for the open-end reflection coefficient with the neglect of the small contribution from radiation damping.

4.2. Overall pressure in the tunnel

The overall perturbation pressure within the tunnel consists of a linear superposition of the incident pressure p_I , the wave p_R reflected from the open end when the presence of the windows is ignored (given to a sufficient approximation by Eq. (2.23)), and the net radiation from each window:

$$p(x, t) = p_I(t - x/c_0) + p_R(t + x/c_0) + \sum_{k=1}^N p_k(x, t). \tag{4.6}$$

This *linear acoustic theory* formula is applicable sufficiently close to the portal that cumulative effects of nonlinearity within the tunnel can be ignored.

Each $p_k(x, t)$ is defined as in Eq. (4.5) by the system of equations

$$\begin{aligned} \bar{\ell}_k(t) \rho_0 \frac{dV_k}{dt} + \frac{\rho_0 V_k |V_k|}{2\sigma^2} &= p_I \left(t - \frac{x_k}{c_0} \right) + p_R \left(t + \frac{x_k}{c_0} \right) + \sum_{j=1}^N p_j(x_k, t), \\ \frac{d\mathcal{L}_k}{dt} &= |V_k(t)|, & k = 1, 2, \dots, N. \\ \bar{\ell}_k(t) &= \frac{\pi R_k}{4} + \left(\ell_w + \frac{\pi R_k}{4} \right) / \left[1 + \frac{1}{3} \left(\frac{\mathcal{L}_k}{2R_k} \right)^{1.585} \right], \end{aligned} \tag{4.7}$$

The *causal* solution is required, subject to $V_k(t) = 0$, $\mathcal{L}_k(t) = 0$ ($k = 1, 2, \dots, N$) for t large and negative.

4.3. One window

Consider first the canonical case of a single, rectangular window with centroid at x_1 and dimensions ℓ_x , ℓ_θ , respectively, in the x and azimuthal directions (see Fig. 5), and cross-sectional area $\mathcal{A}_1 = \ell_x \ell_\theta$. For the purpose of illustration take

$$x_1 = -5R, \quad \ell_x = 0.8R, \quad \ell_\theta = 0.4R, \quad \ell_w = 0.06R. \tag{4.8}$$

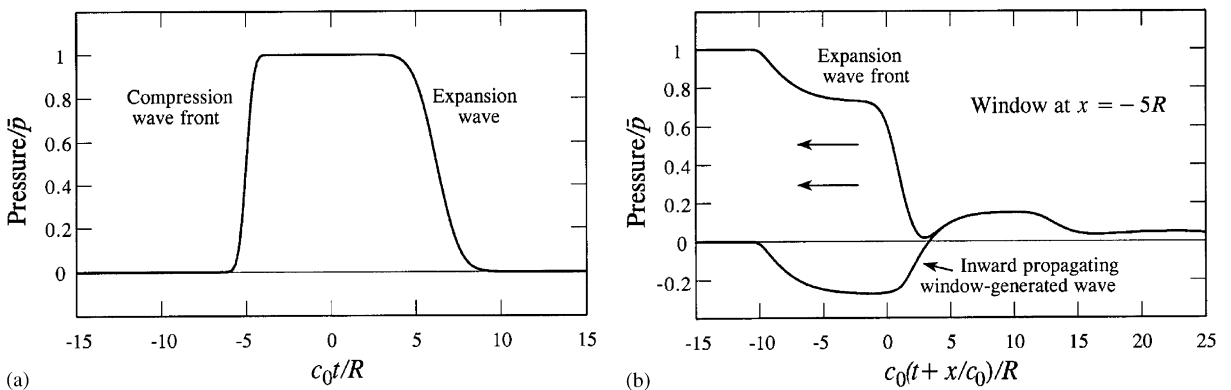


Fig. 6. (a) Pressure history $p_I + p_R$ at the location $x_1 = -5R$ of a ‘closed’ window for an incident compression wave of amplitude $\bar{p} = 4$ kPa and semi-thickness $\delta = 0.5R$. (b) The expansion wavefront and the inward propagating window-generated wave for the window defined by Eq. (4.8).

Let the incident compression wave (2.1) be defined by

$$\bar{p} = 4 \text{ kPa}, \quad \delta \equiv c_0\tau = 0.5R. \tag{4.9}$$

This is a relatively steep wave whose amplitude is typical of that generated by a train entering the other end of the tunnel at about 360 km/h when the tunnel ‘blockage’ ~ 0.2 (Maeda, 2002).

Consider first the situation when the influence of the window is ignored (when the window is ‘closed’). The pressure history at the centroid $x = x_1 = -5R$ of the window then takes the form depicted in Fig. 6(a), equal to

$$p_I\left(t - \frac{x_1}{c_0}\right) + p_R\left(t + \frac{x_1}{c_0}\right).$$

In the figure time is measured from the instant that the midpoint of the compression wavefront arrives at the open end of the tunnel, so that the pressure at the window rises rapidly to \bar{p} at $c_0t/R \approx -5$. The pressure is maintained at this value until the subsequent arrival at $c_0t/R \approx +5$ of the expansion wave reflected at the open end.

When the window is open the incident wave pressure rise at the window produces an outflow that generates a negative pressure pulse $p_1(x, t)$ that propagates in both directions from the window. The component propagating *into* the tunnel is plotted as the lower curve in Fig. 6(b) within the interval $-10 < c_0(t + x/c_0)/R < 3$. At later times the inward propagating wave becomes positive because of reflection and sign change of the window-generated wave at the open end of the tunnel. The combination

$$p_1(x, t) + p_R\left(t + \frac{x_1}{c_0}\right)$$

of this inward propagating pulse and of the reflection of the incident wave from the tunnel portal produces the expansion wavefront shown in Fig. 6(b). The initial drop in pressure at the front of the expansion wave is caused by the inward propagating window pulse $p_1(x, t)$, the subsequent decay to zero by the arrival of p_R from the open end, and the later small rise and fall is produced by reflection of the window-generated wave from the open end and further interactions with the window.

The results shown in Fig. 6 are typical of all ‘one window’ interactions. Variations in the amplitude \bar{p} and thickness 2δ of the incident wave have no significant impact. Increasing the overall area of the window increases the depth of the initial negative window pulse, and therefore the initial drop in pressure at the expansion wavefront. Similarly, the overall time scale (or ‘thickness’) of the negative pulse ($\sim 10R/c_0 = 2|x_1|/c_0$ in Fig. 6(b)) is larger for windows further within the tunnel.

4.4. Multiple windows

A distributed system of windows near the portal can be used to produce a reflected expansion wave with an expansion wavefront that is extensive and smooth. This will be illustrated by cases involving ten windows evenly spaced along the

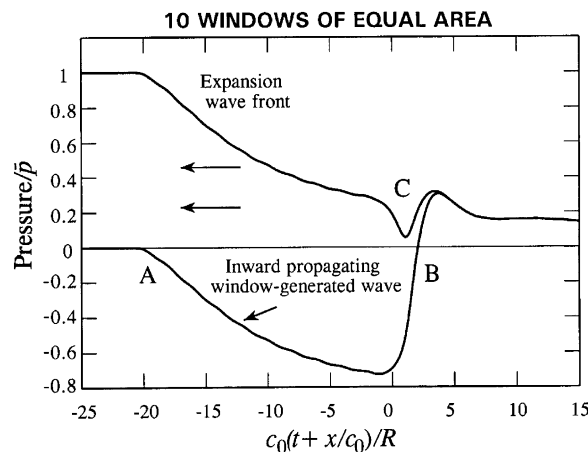


Fig. 7. The expansion wavefront and the inward propagating window-generated wave for Case 1 of 10 equal windows defined by Eq. (4.10); the incident compression wave has amplitude $\bar{p} = 4 \text{ kPa}$ and semi-thickness $\delta = 0.5R$.

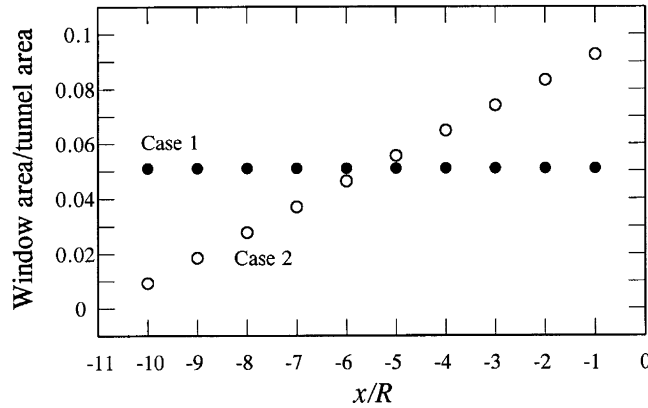


Fig. 8. Uniform and linear window area distributions for Cases 1 and 2.

side of the portal. In Case 1 the windows are square with sides $\ell_x = \ell_\theta = 0.4R$, and we take

$$x_k = -kR, \quad \mathcal{A}_k/\mathcal{A} = 0.16/\pi = 0.0509 \quad (k = 1, 2, \dots, 10), \quad \ell_w = 0.06R. \quad (4.10)$$

Fig. 7 illustrates the form of the expansion wavefront and the overall windows-generated wave radiated into the tunnel (in $x < -10R$), when the incident wave is specified as in Eq. (4.9). The expansion wavefront extends over a wave thickness $\sim 20R$. The negative pressure wave generated by the windows and radiated into the tunnel begins to form at the time $t \sim -10R/c_0$ at which the incident step wave arrives at the first window at $x = x_{10} = -10R$. The front of this window-generated wave ('A' in Fig. 7) marks the front of the extended expansion wave; the further contributions from this window and from other windows closer to the tunnel exit produce the extended negative pressure pulse shown in the figure (between 'A' and 'B'); reflection of the combined pressures of the incident wave and the window generated pressure at the tunnel portal produces (for $t > 0$) the fluctuation 'C' in the expansion waveform together with a low amplitude 'tail' which is similar to that shown in Fig. 6b for one window.

However, for an environmentally ideal reflected wave the pressure *gradient* dp/dt should be constant across the main expansion front (Maeda, 2002; Vardy, 1978; Brown and Vardy, 1994). This ensures that subjectively harmful pressure transients vary relatively *slowly* within the tunnel. The ideal can more nearly be achieved by using an array of windows of variable size. The windows in Case 1 have the uniform window distribution corresponding to the solid circles in Fig. 8. The open circles represent the simplest generalisation in which the window areas decrease linearly with distance into the tunnel, and this is taken to define Case 2:

$$x_k = -kR, \quad \mathcal{A}_k/\mathcal{A} = 0.16(11 - k)/5.5\pi \quad (k = 1, 2, \dots, 10), \quad \ell_w = 0.06R. \quad (4.11)$$

In Case 2 the overall fractional window area $\sum_k \mathcal{A}_k/\mathcal{A} \approx 0.509$ is the same as in Case 1, and the slope of the linear variation has been chosen arbitrarily so that windows in Cases 1 and 2 have roughly the same area near the centroid $x = -5.5R$.

The corresponding reflected waveforms plotted in Fig. 9 are very similar to the corresponding profiles in Case 1, except that the pressure variation across the expansion wavefront is essentially linear over the main region of change. The fluctuation near $c_0(t + x/c_0)/R \sim 0$ and the positive tail at positive retarded times are both similar to those in Case 1.

The magnitude of the fluctuation ('C' in Fig. 7) decreases as the semi-width δ of the incident wave increases. When effective countermeasures (Maeda, 2002) are used to control the profile of the compression wave generated by a train entering the far end of the tunnel, the wave-front thickness 2δ can usually be assumed to exceed, say, $3R$. The expansion wave for this incident wave in Case 2 is shown in Fig. 10. The waveforms are both smoother, because the incident pressure variations occur over distances much larger than the diameter of a typical window, and the fluctuation at 'C' is much diminished.

5. Conclusion

The amplitudes of compression waves generated by a high-speed train within a tunnel can be as large as 3% or 4% of the mean atmospheric pressure. This relatively weak pressure perturbation constitutes a significant disturbance when regarded as sound, to which it is more akin after travelling within a long tunnel and experiencing nonlinear wave

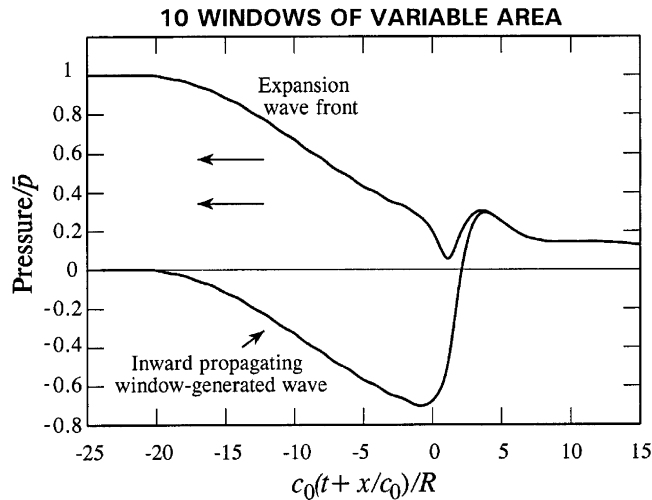


Fig. 9. The expansion wavefront and the inward propagating window-generated wave for Case 2 of 10 windows of variable area defined by Eq. (4.11); the incident compression wave has amplitude $\bar{p} = 4$ kPa and semi-thickness $\delta = 0.5R$.

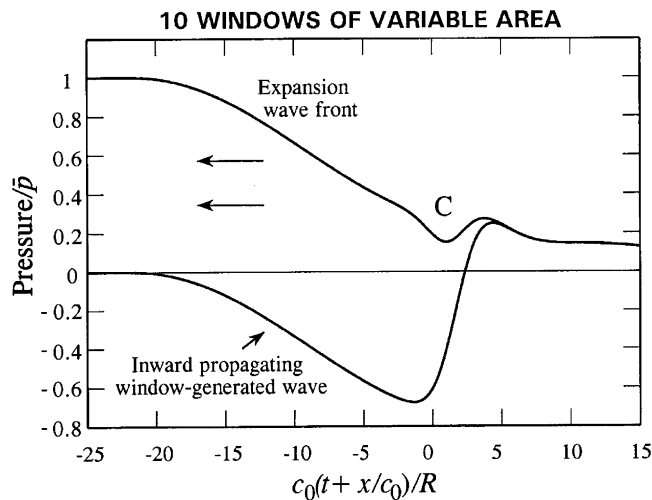


Fig. 10. The expansion wavefront and the inward propagating window-generated wave for Case 2 of 10 windows of variable area defined by Eq. (4.11); the incident compression wave has amplitude $\bar{p} = 4$ kPa and semi-thickness $\delta = 1.5R$.

steepening. The ‘micro-pressure’ pulse radiated from the tunnel portal when a steepened compression wave arrives can be particularly loud and startling, and can rattle structures in nearby buildings. However, it appears from our results in Section 3 that even for the most intense micro-pressure waves encountered in practice, nonlinear effects of propagation outside the tunnel are unlikely to be of any great importance.

The expansion wave reflected back into the tunnel ultimately meets the train within the tunnel and may cause discomfort to passengers and personnel. Our analyses of the expansion wave in this paper are complementary to previous studies reviewed by Maeda (2002) and those of Vardy (1978) and Brown and Vardy (1994), and indicate that the usual long wavelength, one-dimensional wave propagation approximation can be used to study the interaction of steepened waves with a portal, and also with windows distributed along the tunnel wall near the portal. Windows are usually used at a tunnel entrance to inhibit wave steepening in a long tunnel. For tunnels with dual tracks these same windows will interact with an impinging compression wave generated by a train entering at the other end, and produce an expansion wave whose wavefront profile depends on the distribution of the windows and their dimensions. For

single track tunnels in which trains travel in one direction only, our calculations confirm that window size and distribution can be adjusted to reduce the impact of the reflected expansion wave by ensuring that the pressure changes at an approximately constant rate across an extended wavefront whose thickness is many times larger than the front of the incident compression wave.

References

- Abramowitz, M., Stegun, I.A. (Eds.), 1970. *Handbook of Mathematical Functions* (ninth corrected printing). US Department of Commerce, National Bureau of Standards Applied Mathematics Series No. 55.
- Brown, J.M.B., Vardy, A.E., 1994. Reflections of pressure waves at tunnel portals. *Journal of Sound and Vibration* 173, 95–111.
- Chester, W., 1950. The propagation of sound waves in an open ended channel. *Philosophical Magazine* 41, 11–13.
- Cummings, A., 1984. Acoustic nonlinearities and power losses at orifices. *American Institute of Aeronautics and Astronautics Journal* 22, 786–792.
- Cummings, A., 1986. Transient and multiple frequency sound transmission through perforated plates at high amplitude. *Journal of the Acoustical Society of America* 79, 942–951.
- Disselhorst, J.H.M., van Wijngaarden, L., 1980. Flow in the exit of open pipes during acoustic resonance. *Journal of Fluid Mechanics* 99, 293–319.
- Hamilton, M.F., Tjotta, J.N., Tjotta, S., 1985. Nonlinear effects in the farfield of a directive sound source. *Journal of the Acoustical Society of America* 78, 202–216.
- Howe, M.S., 2005. On the role of separation in compression wave generation by a train entering a tunnel hood with a window. *IMA Journal of Applied Mathematics* 70, 400–418.
- Howe, M.S., Iida, M., Fukuda, T., Maeda, T., 2003. Aeroacoustics of a tunnel-entrance hood with a rectangular window. *Journal of Fluid Mechanics* 487, 211–243.
- Iida, M., 2003. Private communication.
- Kuznetsov, V.P., 1971. Equations of nonlinear acoustics. *Soviet Physics Acoustics* 16, 467–470.
- Lee, Y.-S., Hamilton, M.F., 1995. Time-domain modeling of pulsed finite-amplitude sound beams. *Journal of the Acoustical Society of America* 97 (2), 906–916.
- Levine, H., Schwinger, J., 1948. On the radiation of sound from an unflanged circular pipe. *Physical Review* 73, 383–406.
- Lighthill, J., 1978. *Waves in Fluids*. Cambridge University Press, Cambridge.
- Maeda, T., 2002. Micropressure waves radiating from a Shinkansen tunnel portal. In: Krylov, V.V. (Ed.), *Noise and Vibration from High Speed Trains*. Thomas Telford (Chapter 7).
- Morse, P.M., Feshbach, H., 1953. *Methods of Theoretical Physics*, vol. 2. McGraw-Hill, New York.
- Noble, B., 1958. *Methods based on the Wiener–Hopf Technique*. Pergamon Press, London (reprinted 1988, Chelsea Publications, New York).
- Ozawa, S., Maeda, T., 1988a. Tunnel entrance hoods for reduction of micro-pressure wave. *Quarterly Report of the Railway Technical Research Institute* 29 (3), 134–139.
- Ozawa, S., Maeda, T., 1988b. Model experiment on reduction of micro-pressure wave radiated from tunnel exit. In: Emori, R.I. (Ed.), *Proceedings of International Symposium on Scale Modeling*, Tokyo, 18–22 July. Japan Society of Mechanical Engineers, Seikei University, pp. 33–37.
- Ozawa, S., Uchida, T., Maeda, T., 1978. Reduction of micro-pressure wave radiated from tunnel exit by hood at tunnel entrance. *Quarterly Report of the Railway Technical Research Institute* 19 (2), 77–83.
- Ozawa, S., Murata, K., Maeda, T., 1997. Effect of ballasted track on distortion of pressure wave in tunnel and emission of micro-pressure wave. In: Gillard, J.R. (Ed.), *Ninth International Conference on Aerodynamics and Ventilation of Vehicle Tunnels*. Mechanical Engineering Publications Limited, UK.
- Peters, M.C.A.M., Hirschberg, A., Reijnen, A.J., Wijnands, A.P.J., 1993. Damping and reflection coefficient measurements for an open pipe at low Mach and low Helmholtz numbers. *Journal of Fluid Mechanics* 256, 499–534.
- Rayleigh, L., 1926. *The Theory of Sound*, vol. 2. Macmillan, London.
- Rudinger, G., 1955. On the reflection of shock waves from an open end of a duct. *Journal of Applied Physics* 26, 981–993.
- Rudinger, G., 1957. The reflection of pressure waves of finite amplitude from an open end of a duct. *Journal of Fluid Mechanics* 3, 48–66.
- Vardy, A.E., 1978. Reflection of step-wavefronts from perforated and flared extensions. *Journal of Sound and Vibration* 59, 577–589.
- van Wijngaarden, L., 1968. On the oscillations near and at resonance in open pipes. *Journal of Engineering Mathematics* 2, 225–240.
- van Wijngaarden, L., Disselhorst, J.H.M., 1979. Resonant gas oscillations in open pipes. *Archives für Mechanik* 31, 115–124.
- Zabolotskaya, E.A., Khokhlov, R.V., 1969. Quasiplane-plane waves in the nonlinear acoustics of confined beams. *Soviet Physics Acoustics* 15, 35–40.